Polymer Swelling. 19. Sorption of α,ω-Dialkoxy-Substituted Linear Poly(methylenes) and Poly(oxyethylenes) by Poly(styrene-*co*-divinylbenzene)

L. A. Errede* and George V. D. Tiers

3M Corporate Research Laboratories, 3M Center, 201-2N-22, St. Paul, Minnesota 55144

Received: December 18, 1996[⊗]

The adsorption parameters (α) for 10 linear and five branched polyether liquids were established in the usual way.[1−13] These data were then used to deduce the α-values for all the possible structural permutations of the polyethers having general molecular structure (GMS) $H(CH_2)_mO(CH_2)_cOCH_{2-q}(CH_3)_q(CH_2)_{n-1}H$ (in which $m = 1-8$, $n = m$ to 8, $q = 0-2$, and $c = 2-12$) and those having GMS $R'(OCH_2CH_2)_eOR$ (in which $e = 1-5$ and R′ and R are linear and branched alkyl groups) by systematic incrementation of one of the variables *m*, *n*, *q*, *c*, or *e*, the rest being kept constant, as described in the text. The data obtained thereby are consistent with the concept that the diethers are adsorbed asymmetrically to the pendent phenyl groups of poly(styrene-*co*-divinylbenzene) at liquid-saturation, whereas those having more than two oxygen atoms are adsorbed symmetrically thereto.

Introduction

Earlier publications[1] in this series, devoted to studies of liquid sorption by poly(styrene-*co*-divinylbenzene) [hereinafter referred to either as poly(Sty-*co*-DBV) or $(Sty)_{1-x}(DVB)_x$], reported the concept of an adsorption parameter for the sorbed liquid with respect to the sorbent polymer. This parameter is defined as the number (α) of adsorbed molecules per accessible phenyl group in the polymer at liquid-saturation. It can be established gravimetrically, by means of a set of six $(Sty)_{1-x}(DVB)_x$ samples having known values of *x*, as described in considerable detail elsewhere[1−12] and recounted briefly here in the Experimental Section. These α-values reflect very sensitively the molecular structure of the adsorbed species and how it is accommodated by that of the repeat unit in the polymer. The α-values established thus far (>500 in all)[1−12] range from 0 to about 3.7, and they are reproducible to within ±0.01.

In this respect, the adsorption parameter (α) is much more precise than the corresponding Flory−Huggins interaction parameter (χ); nevertheless between these parameters there is good correlation.[13] Hence α can be used advantageously to calculate the corresponding χ to ±0.01 for a given polystyrene liquid system, as described in the Experimental Section, but χ as determined by conventional procedures *cannot* be used meaningfully to calculate the corresponding α, because the usual experimental methods for establishing χ are often reproducible only to ±1 in the first significant figure at that volume fraction ($v = 1$) of the system where χ is most sensitive to the molecular structure of the sorbed species.[13]

Parts 1−18 in this ongoing series[1−12] describe how the relative affinity (as measured by α) of an adsorbed species for the repeat unit of the sorbent polymer reflects very sensitively the molecular structure of that species. Furthermore, by considering homologous series of liquids, it was possible to establish the factors that affect α, such as (1) electronic attraction of the functional group in the sorbed species for the phenyl group in the sorbent polymer, (2) steric hindrance to adsorption owing to the bulkiness of the rest of the molecule in the vicinity of the adsorption site (i.e., the phenyl group of the polymer at liquid-saturation), (3) the manner in which the "adsorbed portion" of the adsorbed species makes liaison with the adsorption site, (4) the approximate angle that the "nonadsorbed portion" of the adsorbed species "above" the adsorption site makes with the hypothetical plane of adsorption, and (5) the magnitude of dynamic interaction of the "nonadsorbed portion" above the adsorption site with the sorbed-but-not-adsorbed molecules in the polymer−liquid gel system at saturation, which necessarily affects the angle of adsorption.

We began these studies using simple linear homologous series,[1−6] namely, those having general molecular structures (GMSs) of the types $Z(CH_2)_{n+1}H$, in which Z is a substituent (such as a chloro, bromo, iodo, or phenyl group) that has strong affinity for the phenyl groups in the polymer, and *n* is an integer from 0 to 7. We then proceeded to considerations of progressively more complicated series,[7−12] such as those having the GMSs of the types $ZCH_{2-q}(CH_3)_q(CH_2)_{n+1}H$ (in which *q* is an integer from 0 to 2) and then to the ethers $H(CH_2)_{m+1}(CH_3)_{q'}CH_{2-q'}OCH_{2-q}(CH_3)_q(CH_2)_{n+1}H$ (in which *m* is an integer from 0 to 7, *n* is an integer from *m* to 7, and *q*′ and *q* are integers from 0 to 2). The sequence in which these studies were published (parts 12−18; refs 7−12, respectively) was not chronologically in accordance with the date of investigation, but rather in the order of complication and ease of understanding, so that the information presented in one publication could be used to interpret properly the observations reported in the next.

We observed, in studies using the ethers having the above GMS,[7,13] that the α-values varied not only with the change in the total number (*N*) of methylene units (or equivalent) in the molecular structure but also in the type of change (i.e., in *m*, *n*, *q*′, or *q*). We noted, however, that when one of these four variables was varied incrementally from its initial value to its allowable limit while the other three were held constant, the logarithms of the α-values for the molecules that comprised that series varied linearly with *N*, as expressed by eq 1.

$$\log \alpha_f = \log \alpha_i - D_s(N_f - N_i) \qquad (1)$$

Here N_f and N_i are the respective final and initial *N* values of the homologous series being considered, α_f and α_i are the corresponding α-values, and D_s is the characteristic decremen-

[⊗] Abstract published in *Advance ACS Abstracts,* April 1, 1997.

S1089-5647(97)00032-1 CCC: $14.00

tation constant (i.e., the decrease in log α per unit increase in *N*) for that series.

Each of these log α *vs N* relationships (eq 1) is in effect a vector, such that the full set of these relationships comprise a self-consistent rigidly interconnected universe of vectors in multidimensional space.[11] When this universe is projected onto a two-dimensional surface, D_s represents the vertical component of the corresponding decrementation constant. Thus, when only two (or more) α-values for members of a given series are determined experimentally, those for the rest of the members in that series can be calculated with reasonable confidence by means of eq 1, as described in considerable detail elsewhere.[10−12] ln was also shown[11] that when dealing with multiple sets of such relationships that intersect one another (i.e., the homologous series that they represent have one or more elements in common), the calculated value for log α_f for any given point, determined from an established log α_i for any other point, is independent of the pathway of travel from the initial point (log α_i:N_i) to the final point (log α_f:N_f), and that the relative difference is given by eq 2.

$$(\log \alpha_i - \log \alpha_f) = \sum_{j=1}^{n} D_j \Delta N_j \qquad (2)$$

Here D_j and ΔN_j represent respectively the decrementation constants and the corresponding displacements along the sequence of vectors chosen to go from point log α_i:N_i to point log α_f:N_f.

When one is dealing with two variables, each of which is incremented systematically while the remaining variables that define the GMS are kept constant, the vectors obtained thereby fall on a plane that is defined by any two intersecting vectors therein (see Figures 3 and 8−14 in ref 11). The rigidly interconnected gridwork of vectors obtained thereby represents two sets of mutually intersecting parallel lines. The points of intersection identify the α-values for all the possible permutations of the GMS represented by that plane.

An example of such a grid system that is very germane to the discussions that will soon follow is reproduced in Figure 1, which is a plot of all the log $\alpha_{m,n}$ *vs N* (the total number of methylene and oxygen mass units in the ether, i.e., $m + n + 1$) relationships for all the homologous series having two or more members that are subsets of the linear aliphatic ethers having the GMS $H(CH_2)_mO(CH_2)_nH$ [i.e., the three sets of six log $\alpha_{m,n}$ *vs N* relationships that are parallel respectively to those for homologous series $CH_3O(CH_2)_nH$, $H(CH_2)_mO(CH_2)_8H$, and $H(CH_2)_mO(CH_2)_mH$]. These relationships define a planar figure (a triangle) in three-dimensional space, and Figure 1 is the projection of that triangle onto a two-dimensional surface, namely, the plane of the paper. The intersection of these three sets of parallel lines identifies the $\alpha_{m,n}$-values (36 in number) for all the possible structural permutations of the ethers having the GMS $H(CH_2)_mO(CH_2)_nH$.

The molecular structures of members of the series that comprise the three sides of the triangle in Figure 1 are identified by the two numbers (*m*,*n*) adjacent to the data point. The first refers to the number of methylene groups in the shorter chain, and the second refers to the corresponding number in the longer chain. The experimentally determined $\alpha_{m,n}$-values that were used to establish the grid system are represented by filled circles. The $\alpha_{m,n}$-values determined for ethers that became available to us subsequently are recorded as empty circles. It is gratifying to note that these later-established experimental $\alpha_{m,n}$-values coincide precisely with the expected locations predicted by their respective points of intersection.

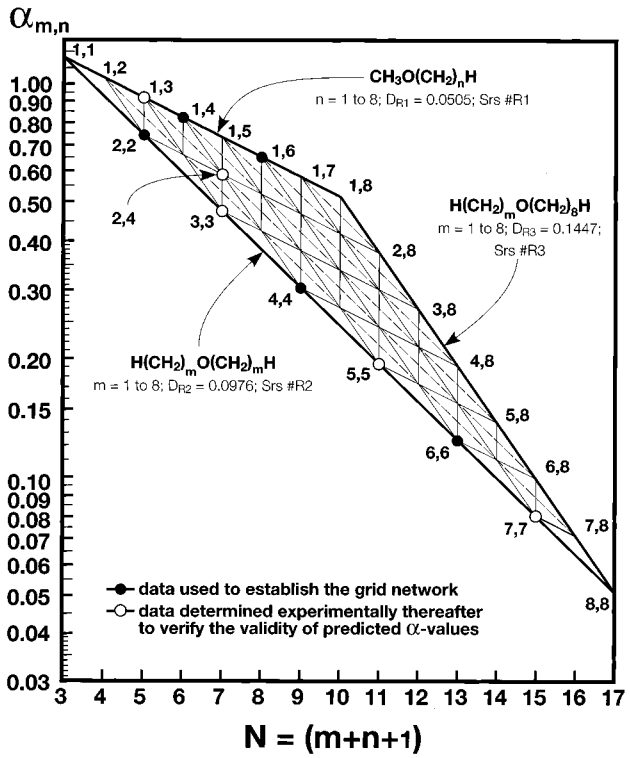

Figure 1. The log α *vs N* linear relationsips for sorption-to-saturation of $H(CH_2)_mO(CH_2)_nH$ liquids by poly(Sty-*co*-DVB); correlation of log $\alpha_{m,n}$ with *N*, the sum of methylene (*m* and *n*) and oxygen (1) mass units in the sorbed ether.

Similar considerations for the corresponding branched series of ethers (i.e., *q* and/or *q*′ are greater than 0) show similar planes-of-vector relationships that intersect the reference plane (Figure 1, in which *q* and *q*′ are both 0), but extend uniformly below it, as shown in Figures 5−12 in ref 11. These results were interpreted to mean that such ethers are not adsorbed symmetrically with respect to the plane of the adsorption site; that is, the smaller, less complicated, alkyl group (R′) of the adsorbed ether (R′OR) lies close to the plane of the adsorption site (i.e. the phenyl group), while the larger alkyl group (R) extends "above" this site and is in dynamic associative interaction with the mobile sorbed-but-not-adsorbed molecules of its own kind in the liquid-saturated system (see Figures 4 in refs 11 and 12).

Our studies of sorption, using polyfunctional liquids having GMSs of the type $CH_{3-z}Z_z(CH_2)_{n+1}H$ and $Z(CH_2)_{n+1}CH_{3-z}Z_z$ (in which Z is chloro,[7] bromo,[7] or an alkoxy group[12] and *n* is an integer from 0 to 7), showed that liaison of such multifunctional molecules with respect to the polymer is monodentate at liquid-saturation. The rest of the Z-substituents are located on the portion of the molecule that extends above the adsorption site, where they can (1) affect the electronic affinity for the adsorption site, (2) affect steric hindrance with respect to that site, and (3) participate in dynamic associative interactions with the mobile molecules of their own kind that comprise the bulk of the sorbed molecules in the polymer liquid system at saturation. Consequently, they affect not only α for the first member of the series being considered but also the decrementation constant of that series (D_s; eq 1). In such cases, log α_z does not vary linearly with *z*, but rather it exhibits maxima that depend on the complicated mode of interaction between the above cited three factors.[12] It was also noted, however, that if the molecular architecture on the carbon atoms having Z-substituents are kept constant while *n* in such series is incremented from 1 to its allowable limit, then log α_n of that series varies linearly with *n* in the normal manner,[12] as expressed by eq 1.

TABLE 1: Adsorption Data for α-Values That Were Determined Experimentally[a]

identification of sorbed liquid			adsorption data				
srs. no.	GMS	E#	d	$\lambda_o^{1/3}$	C	α	χ_1
1	$CH_3O(CH_2)_cOCH_3$						
	$c = 2$	1	0.863	1.70	1.51	1.50	0.58
	$c = 4$	2	0.855	1.86	1.62	1.22	0.51
	$c = 6$	3	0.852	1.93	1.66	1.01	0.49
2	$CH_3OCH_2CH_2O(CH_2)_nH$						
	$n = 1$	1	0.863	1.70	1.51	1.50	0.58
	$n = 2$	4	0.846	1.82	1.52	1.28	0.57
	$n = 4$	5	0.841	1.81	1.44	0.96	0.62
3	$H(CH_2)_mOCH_2CH_2O(CH_2)_mH$						
	$m = 1$	1	0.863	1.70	1.51	1.50	0.58
	$m = 2$	6	0.842	1.80	1.37	1.02	0.66
	$m = 4$	7	0.835	1.71	0.87	0.43	0.97
4	$CH_3OCH_2CH_2OCH_{2-q}(CH_3)_qCH_3$						
	$q = 0$	4	0.846	1.82	1.52	1.28	0.57
	$q = 2$	8	0.840	1.81	1.19	0.79	0.77
5	$H(CH_2)_2OCH_2CH_2OCH_{2-q}(CH_3)_qCH_3$						
	$q = 0$	6	0.842	1.80	1.37	1.02	0.66
	$q = 2$	9	0.834	1.80	0.94	0.56	0.93
6	$H(CH_2)_mO[CH_2CH_2O]_2(CH_2)_mH$						
	$m = 1$	10	0.937	1.79	1.40	1.02	0.65
	$m = 2$	11	0.909	1.70	1.37	0.80	0.66
	$m = 4$	12	0.885	1.79	1.13	0.48	0.81
7	$CH_3O[CH_2CH_2O]_2C(CH_3)_3$	13	0.909	1.89	1.31	0.70	0.70
8	$CH_3O[CH_2CH_2O]_eCH_3$						
	$e = 1$	1	0.863	1.70	1.51	1.50	0.58
	$e = 2$	10	0.937	1.79	1.40	1.02	0.65
	$e = 3$	14	0.986	1.72	1.29	0.74	0.71
	$e = 4$	15	1.009	1.74	1.21	0.57	0.76

[a] srs. no. is the identification number of the series. E# is the identification number of the ether liquid. d is the density of the liquid. λ_o is the value of λ extrapolated to $S = 0$, as defined in eq 2. C is the relative swelling power of the liquid, as defined in eq 2. α is the adsorption parameter of the liquid, as defined in eq 3. χ_1 is the Flory−Huggins interaction parameter (χ_ν at $\nu = 1$), which was calculated from C, using eqs 4 and 5.

It was now of interest to test whether or not the above observations can be extended to the (α,ω-dialkyl-linear)-diethers having the GMSs $R'O(CH_2)_cOR$, in which c is an integer from 2 to 12, or the corresponding polyethers $R'O(CH_2CH_2O)_eR$, in which e is an integer from 1 to about 6. The purpose of this publication, therefore, is to report the results of this investigation and the conclusions derived therefrom.

Experimental Section

The set of six composite film samples, employed as the polymeric sorbent in all our previous studies of $(Sty)_{1-x}(DVB)_x$ swelling-to-saturation in a test liquid,[1−12] were used again in the present studies of swelling in polyalkoxy-substituted polymethylenes and poly(oxyethylenes). The procedure for making these composite film samples, comprised of $(Sty)_{1-x}(DVB)_x$ particles (>80% by weight) enmeshed in PTFE microfibers, and the distribution of these particles in the microporous composite films produced thereby (see Figures 1, 6, 7, and 20 of ref 1) are described in considerable detail elsewhere.[1−12] This set of samples, each containing microparticles having a known value of x (i.e., $x = 0.01$, 0.02, 0.03, 0.04, 0.08, or 0.11), were allowed to swell to saturation in the test liquid at 23 ± 1 °C. Reagent grade samples of most of these liquids were obtained from commercial sources, and they were used as such without further purification. Exceptions are the samples of 1,4-dimethoxy-*n*-butane, 1,6-dimethoxy-*n*-hexane, 1-methoxy-4-ethoxyethane, and 1-methoxy-4-*n*-butoxyethane (i.e., ethers nos. 2−5 in Table 1), which were synthesized and purified by fractional distillation in our laboratory, as described elsewhere.[14]

The volumes (S) of sorbed liquid, per gram of enmeshed particles, in these samples were determined gravimetrically in the usual way.[1−12] The slope of the straight line obtained when the S-values are plotted as a function of the corresponding cube root of the average number [λ; i.e., the ratio $(1 + x)/x$ calculated for the sample having the average composition $(Sty)_{1-x}(DVB)_x$] of backbone carbon atoms between cross-link junctions in the respective samples indicates the relative swelling power (C, in mL of adsorbed liquid per gram of particles) of the sorbed test liquid in accordance with eq 3.

$$S = C(\lambda^{1/3} - \lambda_0^{1/3}) \tag{3}$$

Here λ_0 is the value of λ extrapolated to $S = 0$. The corresponding adsorption parameter (α) was calculated from the observed C-values by means of eq 4:

$$\alpha = 104Cd/M \tag{4}$$

The letters d and M refer to the density and formula weight respectively of the test liquid.

The Flory−Huggins interaction parameter (χ_v) is also calculated from C by means of eq 5, as described elsewhere.[13]

$$\chi_v = 0.49 + 1.01\upsilon - 0.61\upsilon C \tag{5}$$

Here υ is the volume fraction of polymer in the polystyrene liquid system. Since it was noted that χ_v is most sensitive to the molecular structure of the sorbed species at $\upsilon = 1$ (see Figure 4 of ref 13), only the χ_1-values are reported in Table 1. The χ_v-values at any other value of υ can be calculated by the interested reader using eq 6.

$$\chi_v = 0.49 + \upsilon(\chi_1 - 0.49) \tag{6}$$

Results and Discussion

Accumulation of Relevant α-Values. The data determined experimentally thus far in our studies involving sorption of α,ω-dialkoxy-substituted polymethylenes and poly(oxyethylenes) by poly(Sty-*co*-DVB) are collected in Table 1. These data are

TABLE 2: α-Values for the Full Set of Members That Comprise Series Nos. 1−6 (Table 1)[a]

identification of the liquid ether			$\log \alpha_f = \log \alpha_i - D(N_f - N_0)$			
srs. no.	formula	E#	α_i	D	N_f	α_f
1	$CH_3O(CH_2)_cOCH_3$					
	$c = 2$	1	1.50	0.0429	6	**1.50**
	$c = 3$	1a		($r^2 = 0.9993$)	7	1.36
	$c = 4$	2			8	**1.22**
	$c = 5$	2a			9	1.11
	$c = 6$	3			10	**1.01**
	$c = 7$	3a			11	0.92
	$c = 8$	3b			12	0.83
	$c = 9$	3c			13	0.75
	$c = 10$	3d			14	0.68
	$c = 11$	3e			15	0.62
	$c = 12$	3f			16	0.56
2	$CH_3OCH_2CH_2O(CH_2)_nH$					
	$n = 1$	1	1.50	0.0643	6	**1.50**
	$n = 2$	4		($r^2 = 0.9994$)	7	**1.28**
	$n = 3$	4a			8	1.12
	$n = 4$	5			9	**0.96**
	$n = 5$	5a			10	0.83
	$n = 6$	5b			11	0.72
	$n = 7$	5c			12	0.62
	$n = 8$	5d			13	0.53
3	$H(CH_2)_mOCH_2CH_2O(CH_2)_mH$					
	$m = 1$	1	1.50	0.0909	6	**1.50**
	$m = 2$	6		($r^2 = 0.9996$)	8	**1.02**
	$m = 3$	6a			10	0.64
	$m = 4$	7			12	**0.43**
	$m = 5$	7a			14	0.28
	$m = 6$	7b			16	0.18
	$m = 7$	7c			18	0.12
	$m = 8$	7d			20	0.080
4	$CH_3OCH_2CH_2OCH_{2-q}(CH_3)_qCH_3$					
	$q = 0$	4	1.28	0.1048	7	**1.28**
	$q = 1$	4a′			8	1.01
	$q = 2$	8			9	**0.79**
5	$CH_3CH_2OCH_2CH_2OCH_{2-q}(CH_3)_qCH_3$					
	$q = 0$	6	1.02	0.1302	8	**1.02**
	$q = 1$	6a			9	0.76
	$q = 2$	9			10	**0.56**
6	$H(CH_2)_mO[CH_2CH_2O]_2(CH_2)_mH$					
	$m = 1$	10	1.02	0.0547	9	**1.02**
	$m = 2$	11		($r^2 = 0.9999$)	11	**0.80**
	$m = 3$	11a			13	0.62
	$m = 4$	12			15	**0.48**
	$m = 5$	12a			17	0.37
	$m = 6$	12b			19	0.29
	$m = 7$	12c			21	0.23
	$m = 8$	12d			23	0.18

[a] srs. no. and E# are as defined in the footnotes of Table 1. α_i is the adsorption parameter for the initial member of the series. α_f is the adsorption parameter being calculated. N_f is the corresponding total number of mass units. D is the decrementation constant, i.e., the negative slope of the best straight line through the set of three data points determined experimentally (bold numerals), and r^2 is the corresponding square of the correlation coefficient for that relationship.

classified into eight homologous series identified by "general molecular structure" (GMS). Each member of a given GMS is identified further by a number (E#, from 1 to 15) in the sequence that they are first recorded in Table 1. Since a given ether may appear in two or more of the eight series therein, it retains in subsequent series the previous E#.

The decrementation constants (D_s; eq 1) for these series were established on the basis of the α-values reported in Table 1. In those cases (series nos. 1, 2, 3, and 6) in which the α-values of three members of the series were determined experimentally (represented in Table 2 by bold numerals), the corresponding D_s-value for that series was calculated from the slope of the best straight line through the set of these three data points. The square of the correlation constant for each of these straight lines of best fit was in all cases $r^2 > 0.9993$, as recorded in Table 2. In those cases that α-values for only two of its members were determined experimentally (series nos. 4 and 5), the corresponding D_s-value is given by the ratio $(\log \alpha_i - \log \alpha_f)/(N_f - N_i)$.

The α-values for the remaining members of srs. nos. 1−6 (Table 1) that were not determined experimentally were calculated by means of eq 1, using the appropriate experimentally determined values for the constants α_i and D_s. The calculated values obtained thereby are recorded in Table 2. The identification scheme for these ethers takes the number for the preceding member having an α-value that was determined experimentally (recorded in bold numerals), further qualified by a lower case letter, which was assigned in the alphabetic sequence of its occurrence, as noted in series nos. 1−6 in Table 2.

The log α *vs N* Relationships for Subsets of $RO(CH_2)_cOR'$ Ethers. The data recorded in Tables 1 and 2 were used to deduce a rigidly interconnected network of log α *vs N* relationships in multidimensional space that represent subsets of homologous series having GMS $H(CH_2)_mO(CH_2)_c$-$OCH_{2-q}(CH_3)_q(CH_2)_{n-1}H$. The protocol for doing so was essentially the same as that used to derive the network that

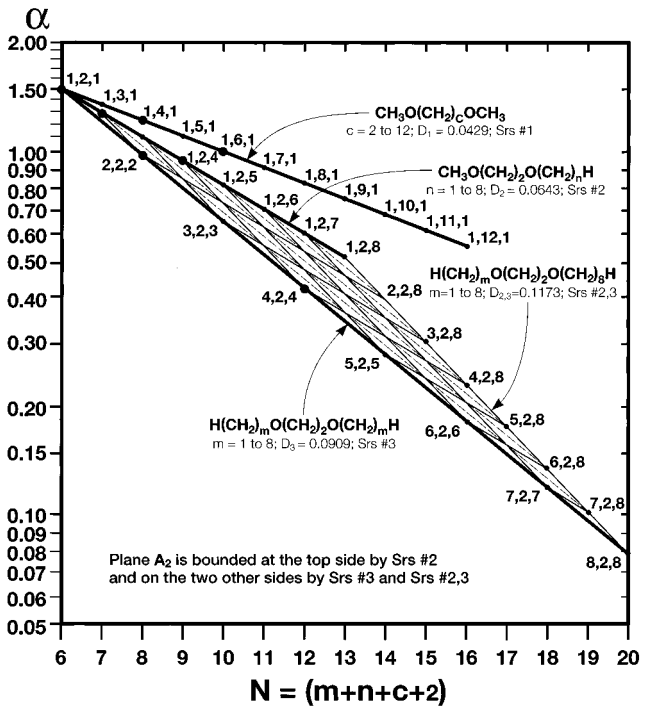

Figure 2. The log α *vs N* linear relationships for sorption-to-saturation of $H(CH_2)_mO(CH_2)_cO(CH_2)_nH$ liquids by poly(Sty-*co*-DVB); correlation of log $\alpha_{m,c,n}$ with *N*, the sum of methylene (*m*, *c*, and *n*) and oxygen (2) mass units in the sorbed ether.

represents those having GMS $H(CH_2)_mOCH_{2-q}(CH_3)_q(CH_2)_{n-1}H$, as outlined in Figures 5 to 14 in ref 11. It was reasoned that a comparison of these two networks should show the qualitative similarities and the quantitative differences that reflect the influence of the second ether oxygen atom in the diether series on α, and also the mitigating effect of *c*, i.e., the distance of the second oxygen atom away from the one that is immobilized by liaison with the adsorption site, as will be explained in the paragraphs that follow.

The α-values for the ethers that comprise srs. nos. 1, 2, and 3 (Table 2) are correlated in Figure 2 with *N* (i.e., $m + n + q + o$; here *q* is 0 and *o*, the number of ether oxygen atoms, is 2). The log α *vs N* relationships for srs. 2 & 3 (the two lower bold straight lines in Figure 2) define two sides of the triangular plane (plane A_2) that contains the log α *vs N* relationships for all the subsets of $H(CH_2)_mO(CH_2)_2O(CH_2)_nH$. The third side of plane A_2 is given by the relationship for $H(CH_2)_mO(CH_2)_2O(CH_2)_8H$ (i.e., *m* incremented from 1 to 8; srs. nos. 2, 3; Table 3). The molecular structures for the ethers, the log α-values for which define the perimeters of this triangular plane, are identified in Figure 2 by the three numbers (*m*,2,*n*) adjacent to the respective data points.

The three sets of intersecting parallel lines within plane A_2 represent the log α *vs N* relationships for the six subsets of $H(CH_2)_mO(CH_2)_2O(CH_2)_nH$ [$m = 2-7$] parallel to that for $CH_3O(CH_2)_2O(CH_2)_nH$ [srs. no. 2; $D_2 = 0.0643$], the six subsets [$n = 2-7$] parallel to that for $H(CH_2)_mO(CH_2)_2O(CH_2)_8H$ [srs. nos. 2, 3; $D_{2,3} = 0.1173$], and the six subsets [$m = n$] parallel to that for $H(CH_2)_mO(CH_2)_2O(CH_2)_mH$ [srs. no. 3; $D_3 = 0.0909$]. The intersections of these three sets of parallel lines (Figure 2) identify the $\alpha_{m,2,n}$-values for all the possible permutations (36) of $H(CH_2)_mO(CH_2)_2O(CH_2)_nH$, the same number as comprises the corresponding set of $H(CH_2)_mO(CH_2)_nH$ ethers (Figure 1).

As expected, the sets of log α *vs N* relationships that comprise plane $\mathbf{A}_0$ in Figure 1 show a striking qualitative similarity to those that comprise plane $\mathbf{A}_2$ in Figure 2 [here the subscripts 0

TABLE 3: The log α *vs N* Relationships Recorded in Figures 2 and 3, Which Were Deduced from the Data Reported in Tables 1 and 2[a]

identification of the liquid ether			$\log \alpha_f = \log \alpha_i - D(N_f - N_0)$			
srs. no.	formula	E#	α_i	D	N_f	α_f
2,3	$H(CH_2)_mOCH_2CH_2O(CH_2)_8H$					
	$m = 2$	5d	0.53	0.1173	13	**0.53**
	$m = 2$	5da			14	0.41
	$m = 3$	5db			15	0.31
	$m = 4$	5dc			16	0.24
	$m = 5$	5dd			17	0.18
	$m = 6$	5de			18	0.14
	$m = 7$	5df			19	0.11
	$m = 8$	7d			20	**0.080**
1A	$CH_3O(CH_2)_cO(CH_2)_8H$					
	$c = 2$	5d	0.53	0.0429	13	**0.53**
	$c = 3$	5da′			14	0.48
	$c = 4$	5db′			15	0.44
	$c = 5$	5dc′			16	0.40
	$c = 6$	5dd′			17	0.36
	$c = 7$	5de′			18	0.32
	$c = 8$	5df′			19	0.29
	$c = 9$	5dg′			20	0.27
	$c = 10$	5dh′			21	0.24
	$c = 11$	5di′			22	0.22
	$c = 12$	5dj′			23	0.20
1B	$H(CH_2)_8O(CH_2)_cO(CH_2)_8H$					
	$c = 2$	7d	0.080	0.0429	20	**0.080**
	$c = 3$	7da			21	0.073
	$c = 4$	7db			22	0.066
	$c = 5$	7dc			23	0.060
	$c = 6$	7dd			24	0.054
	$c = 7$	7de			25	0.049
	$c = 8$	7df			26	0.044
	$c = 9$	7dg			27	0.040
	$c = 10$	7dh			28	0.036
	$c = 11$	7di			29	0.033
	$c = 12$	7dj			30	0.030
2A	$CH_3O(CH_2)_{12}O(CH_2)_nH$					
	$n = 1$	3f	0.56	0.0643	16	**0.56**
	$n = 2$	3fa			17	0.48
	$n = 3$	3fb			18	0.42
	$n = 4$	3fc			19	0.36
	$n = 5$	3fd			20	0.31
	$n = 6$	3fe			21	0.27
	$n = 7$	3ff			22	0.23
	$n = 8$	5dj			23	**0.20**
3A	$H(CH_2)_mO(CH_2)_{12}O(CH_2)_mH$					
	$m = 1$	3f	0.56	0.0909	16	**0.56**
	$m = 2$	3fg			18	0.37
	$m = 3$	3fh			20	0.24
	$m = 4$	3fi			22	0.16
	$m = 5$	3fj			24	0.11
	$m = 6$	3fk			26	0.069
	$m = 7$	3fl			28	0.045
	$m = 8$	7dj			30	**0.030**
2,3A	$H(CH_2)_mO(CH_2)_{12}O(CH_2)_8H$					
	$m = 1$	5dj′	0.20	0.1173	23	**0.20**
	$m = 2$	5dj′a			24	0.15
	$m = 3$	5dj′b			25	0.12
	$m = 4$	5dj′c			26	0.089
	$m = 5$	5dj′d			27	0.068
	$m = 6$	5dj′e			28	0.052
	$m = 7$	5dj′f			29	0.039
	$m = 8$	7dj			30	**0.030**
5A	$H(CH_2)_mOCH_2CH_2OCH(CH_3)_2$					
	$m = 1$	4a	1.01	0.1235	8	**1.01**
	$m = 2$	6a			9	**0.76**
	$m = 3$	6ab			10	0.57
5B	$H(CH_2)_mOCH_2CH_2OC(CH_3)_3$					
	$m = 1$	9	0.79	0.1494	9	0.79
	$m = 2$	10			10	**0.56**
	$m = 3$	10a			11	0.397
	$m = 4$	10b			12	0.281

[a] srs. no., E#, α_i, α_f, and N_f are as defined in the footnotes of Table 2. *D* was calculated using two data points (bold numerals) established in a previous series.

and 2 refer to the number (c) of methylene groups in the internal spacer $\{(CH_2)_cO\}$ that separates the adsorbed portion $\{H(CH_2)_mO\}$ from the nonadsorbed portion $\{(CH_2)_nH$, plus the spacer$\}$]. It is noticed, however, that the α-values for the ethers that comprise plane $\mathbf{A}_2$ [from $\alpha_{1,2,1} = 1.50$ at $N = 6$ to $\alpha_{8,2,8} = 0.080$ at $N = 20$ in Figure 2] are uniformly greater in value than those for the corresponding structures in plane $\mathbf{A}_0$ [from $\alpha_{1,0,1} = 1.18$ at $N = 3$ to $\alpha_{8,0,8} = 0.051$ at $N = 17$ in Figure 1]. This marked difference in α-values that comprise these two triangular planes is attributed to the ether oxygen atom in the nonadsorbed portion $[(CH_2)_2O(CH_2)_nH]$ of the adsorbed diether, which is involved in dynamic interaction "above" the adsorption site with the mobile sorbed-but-not-adsorbed ether molecules in the gel-system at liquid-saturation, as discussed in ref 10. This interaction serves to elevate the nonadsorbed portion to a position of greater "verticality", which lessens steric impedance to further adsorption of other molecules at a given adsorption site (see Figure 4 in ref 10), and thus favors more efficient packing of adsorbed molecules per adsorption site; that is, it causes an increase in α, despite the increase in mass (N) of the adsorbed molecule.

It is also noticed that insertion of the spacer $(CH_2)_2O$ between $H(CH_2)_mO$ and $(CH_2)_nH$ caused a decrease in the area [(Δ log α) *vs* (ΔN)] of plane $\mathbf{A}_2$ (Figure 2) from that for plane $\mathbf{A}_0$ (Figure 1). This decrease in area reflects the increase in the negative slope for the log α *vs* N relationships that define the top sides of these two triangular planes (i.e., from $D_{R1} = 0.0505$ in plane $\mathbf{A}_0$ to $D_2 = 0.0643$ in plane $\mathbf{A}_2$) and the corresponding decreases in negative slopes for those that define the other two sides (i.e., from $D_{R2} = 0.0976$ in plane $\mathbf{A}_0$ to $D_3 = 0.0909$ in plane $\mathbf{A}_2$ and from $D_{R3} = 0.1447$ in plane $\mathbf{A}_0$ to $D_2 = 0.1173$ in plane $\mathbf{A}_2$). These changes in slopes show that the difference in the negative influence on log α per unit increase in m (relative to that per unit increase in n) become less when the distance from the adsorbed portion $H(CH_2)_mO$ to the nonadsorbed portion $(CH_2)_nH$ of the adsorbed ether molecule is increased by insertion of the spacer $(CH_2)_2O$. This is further attributable to the presence of the second ether oxygen, which serves to "lift" the nonadsorbed portion to a position of greater "verticality".

Although it is not yet understood why the above structural modification also serves to mitigate the negative effect on log α per unit increase in m, the increase in the decrementation constant from $D_{R1} = 0.0505$ for $CH_3O(CH_2)_nH$ to $D_2 = 0.0643$ for $CH_3O(CH_2)_2O(CH_2)_nH$ can be rationalized on the basis of the expected greater flexibility that is imparted to the nonadsorbed portion by the presence of the ether oxygen atom. Thus the $(CH_2)_nH$ group can swivel around the second ether atom more effectively than can be attached $(CH_2)_2O$ segment, which is also tethered to the anchor site, and therefore the terminal segment (n) imparts greater steric impedance to adsorption per methylene group than it does in the absence of the spacer segment. That this is indeed the case is supported by the observation that the slope of the log α *vs* N relationships for the subseries of $H(CH_2)_mO(CH_2)_cO(CH_2)_nH$ in which m and n are kept constant while c is incremented from 2 to 12 ($D_1 = 0.0429$ in Figure 2) is less than those ($D_{R1} = 0.0505$ in Figure 1 and $D_2 = 0.0643$ in Figure 2) in which m and c are kept constant while n is incremented from 1 to 8.

The reader is reminded that Figure 2 is a two-dimensional representation of a multidimensional network and that the vector representing srs. no. 1 (topmost bold straight line in Figure 2) is not in plane $\mathbf{A}_2$, which is defined by the lower bold straight lines in Figure 2. The data that comprise srs. no. 1 and plane $\mathbf{A}_2$ can now be used to deduce most of the rigidly interconnected

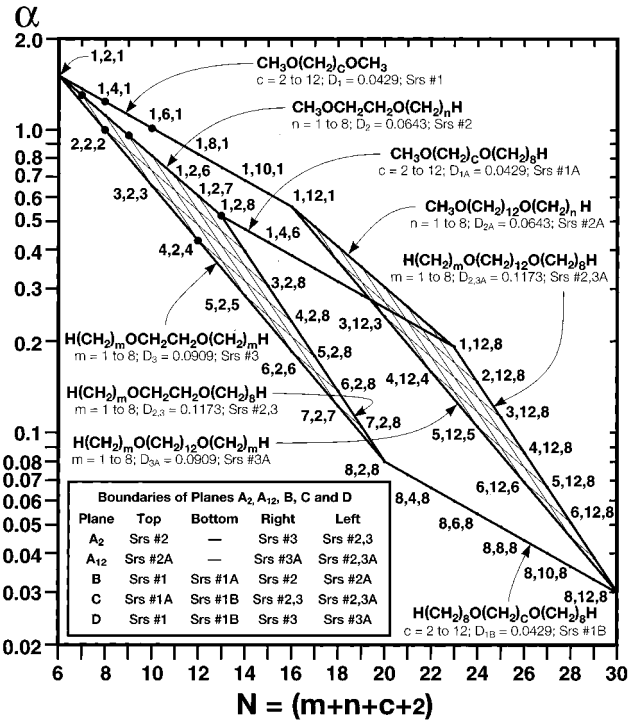

Figure 3. Two-dimensional representation of the three-dimensional space occupied by the log α *vs* N linear relationships of the type noted in Figure 2 that are bounded by two triangular planes ($\mathbf{A}_2$ and $\mathbf{A}_{12}$) and three rectangular planes (**B**, **C**, and **D**), as defined in the tabular inset.

multidimensional network of log α *vs* N relationships for the subseries of $H(CH_2)_mO(CH_2)_cOCH_{2-q}(CH_3)_q(CH_2)_{n-1}H$, in the manner described in considerable detail for $H(CH_2)_mOCH_{2-q}(CH_3)_q(CH_2)_{n-1}$ (see Figures 4−14 in ref 11).

A portion of this network is shown in Figure 3, which was deduced by analogy with the principles observed to be valid in earlier studies[11,12] using the data recorded in Figure 2. The decrementation constants for the log α *vs* N relationships (eq 1) that represent $CH_3O(CH_2)_cOCH_2)_8H$ and $H(CH_2)_8O(CH_2)_cO(CH_2)_8H$ [srs. nos. 1A and 1B, respectively] are assumed to be the same as that ($D_1 = 0.0429$) for $CH_3O(CH_2)_cOCH_3$ [srs. no. 1], since the molecular architecture of the two carbon atoms adjacent to the ether oxygen atom making liaison with the adsorption site is not affected by incrementation of c from 2 to 12, as indicated by several analogous examples described in parts 17 and 18 of this series.[11,12] Hence, the α-values for the ethers that comprise srs. nos. 1A and 1B can be calculated by means of eq 1, using $D_1 = 0.0429$ and the appropriate α_i (i.e., $\alpha_{1,2,8}$ for srs. no. 1A and $\alpha_{8,2,8}$ for srs. no. 1B). These data are recorded in Table 3.

Similarly and for the same reason, D_{3A} for $H(CH_2)_mO(CH_2)_{12}O(CH_2)_mH$ [srs. no. 3A] is assumed to be the same as that ($D_3 = 0.0909$) for the ethers having the GMS $H(CH_2)_mO(CH_2)_2O(CH_2)_mH$ [srs. no. 3]. Consequently, the α-values for the ethers that comprise srs. no. 3A can be calculated by means of eq 1, using $D_3 = 0.0909$ and the appropriate α_i (i.e., $\alpha_{1,12,1}$), as recorded in Table 3. The log α *vs* N relationship for $CH_3O(CH_2)_{12}O(CH_2)_nH$ [srs. no. 2A] is given by the line drawn from point "log $\alpha_{1,12,1}$ at $N = 16$" to point "log $\alpha_{1,12,8}$ at $N = 23$". The log α *vs* N relationship for the ethers having GMS $H(CH_2)_mO(CH_2)_{12}O(CH_2)_8H$ [srs. nos. 2, 3A] is given by the line drawn from point "log $\alpha_{1,12,8}$ at $N = 23$" to point "log $\alpha_{8,12,8}$ at $N = 30$". As expected, the slopes of these two lines agree very well respectively with those representing the GMSs $CH_3O(CH_2)_2O(CH_2)_nH$ [srs. no. 2; $D_2 = 0.0643$] and $H(CH_2)_mO(CH_2)_2O(CH_2)_8H$ [srs. nos. 2, 3; $D_{2,3} = 0.1173$].

The above set of nine log α *vs N* relationships (Figure 3) define the perimeters of the outer five planes of an imaginary three-dimensional structure, which evokes the image of a very flat "roof-section" that could rest atop a narrow rectangular-shaped "house", as outlined in the tabular inset in Figure 3. Not shown in Figure 3 are the set of nine planes ($\mathbf{A}_3$ to $\mathbf{A}_{11}$) that are parallel to planes $\mathbf{A}_2$ and $\mathbf{A}_{12}$ and pass respectively through the set of points for log $\alpha_{1,3,1}$ at $N = 7$ to log $\alpha_{1,11,1}$ at $N = 15$ and the set of six planes ($\mathbf{D}_2$ to $\mathbf{D}_7$) that are parallel to plane **D** and pass respectively through the set of points for log $\alpha_{1,2,2}$ at $N = 7$ to log $\alpha_{1,2,7}$ at $N = 12$. The intersections of these two sets of parallel planes within the imaginary three-dimensional structure shown in Figure 3 identify the $\alpha_{m,c,n}$-values for all the possible permutations of the ethers having GMS $H(CH_2)_mO(CH_2)_cO(CH_2)_nH$ for values of *m* and *n* from 1 to 8 and values of *c* from 2 to 12 (i.e., 396 in all).

The imaginary three-dimensional structure that contains the log $\alpha_{m,2,q,n}$ *vs N* relationships representing subseries of $H(CH_2)_mO(CH_2)_cOCH_{2-q}(CH_3)_q(CH_2)_{n-1}H$ can be deduced as described in considerable detail for the corresponding monoethers, i.e., $H(CH_2)_mOCH_{2-q}(CH_3)_q(CH_2)_{n-1}H$, using the data recorded in Table 3 for ser. nos. 5A and 5B. The set of eight planes for $m = 1-8$, defined by the log $\alpha_{m,2,q,n}$ *vs N* relationships, in which *n* is varied within its allowable limits while *q* is kept constant at 0, 1, or 2 (as shown for example in Figure 9 of ref 11), are joined to the reference plane (plane $\mathbf{A}_2$) at the lines representing the log $\alpha_{m,2,n}$ *vs N* relationships for the diethers $H(CH_2)_mO(CH_2)_2O(CH_2)_nH$ in which *m* is constant at 1−8 while *n* is varied from *m* to 8, such that the imaginary three-dimensional structure obtained thereby evokes the image of a "boat", as shown for example in Figure 10 of ref 11. This mathematical exercise serves to identify the $\alpha_{m,2,q,n}$-values for an additional 72 permutations of $H(CH_2)_mO(CH_2)_2$-$OCH_{2-q}(CH_3)_q(CH_2)_{n-1}H$. Since there are 10 additional equivalent three-dimensional imaginary structures for each incrementation in *c* from 3 to 12 (which are interpenetrating or mutually overlapping), the total number of additional $\alpha_{m,2,q,n}$-values for structural permutations of these diethers that can be estimated by this exercise is 72 × 11 or 792.

Unlike the predicted $\alpha_{m,q,n}$-values for the permutations of the monoethers having GMS $H(CH_2)_mOCH_{2-q}(CH_3)_q(CH_2)_{n-1}H$, most of which are less than $\alpha = 0.1$, the $\alpha_{m,2,q,n}$-values for the diethers $H(CH_2)_mO(CH_2)_2OCH_{2-q}(CH_3)_q(CH_2)_{n-1}H$ are for the most part greater than $\alpha = 0.1$. This means that it will be possible to test easily and with confidence the validity of the values predicted for the diethers, when these ethers become available to us in amounts suitable for experimental measurements, as described in the Experimental Section. In contrast it is considerably more difficult to do so for the monoethers, because the sensitivity and reproducibility of the swelling procedure decreases significantly when α is less than 0.1, and therefore multiple replication and remeasurements over very long time intervals are required to ensure that swelling equilibrium has been established.

The log α *vs N* Relationships for Subsets of $H(CH_2)_m(OCH_2CH_2)_eO(CH_2)_mH$. The above results are consistent with the point of view that the mode of adsorption for these linear-polyether liquids to the sorbent polymer at liquid-saturation is monodentate rather than polydentate and that the remaining ether oxygen atoms are in the "nonadsorbed" portion of the adsorbed molecule that extends away from the adsorption site because these nonadsorbed ether oxygen atoms are in dynamic association with the mobile-but-not-adsorbed ether molecules in the system. These associations serve to increase the "verticality" of the nonadsorbed portion with respect to the plane of the adsorption site and thus to improve how well the molecular structure of the adsorbed molecule is accommodated by that of the repeat unit in the polymer, as described in the Introduction and as reported in ref 12.

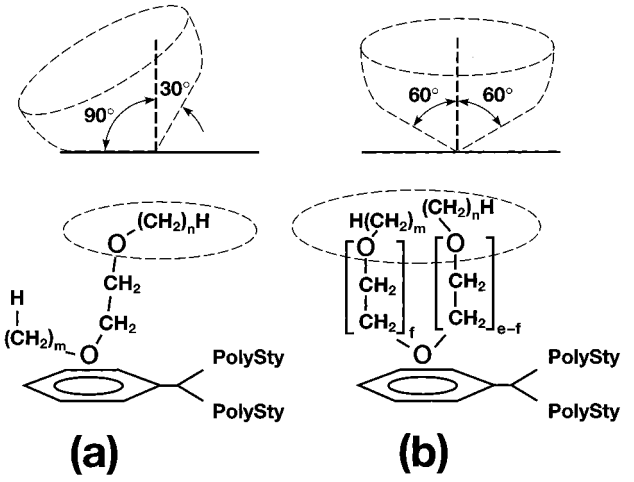

Figure 4. Schematic representation of two modes for adsorption of poly(oxyethylene) ethers $H(CH_2)_mO(CH_2CH_2O)_e(CH_2)_nH$: (a) asymmetric when *e* is 0 or 1, (b) symmetric when *e* is > 1.

The earlier studies using polyether liquids showed that the adsorption preference, with respect to the set of available ether oxygen atoms in the molecular structure, is quite selective and that this selectivity is based on the molecular architecture attained on adsorption that will afford the least amount of steric hindrance to further adsorption at that site and also maximal dynamic association with the mobile sorbed-but-not-adsorbed molecules in the gel system at saturation. For example, the oxygen atom in the homologous series of diethers $H(CH_2)_mO(CH_2)_cO(CH_2)_nH$ [in which *m* is 1−8, *n* is *m* to 8, and *c* is 1−12] that is actually making liaison with the pendent phenyl group of the sorbent polymer is the one that is attached to $H(CH_2)_m$, because this group is smaller than the $(CH_2)_nH$ attached to the alternative oxygen at the other extremity of the linear ether. This selection imparts less steric impedance to further adsorption than does the alternate possibility. In the case of the polyethers having the GMS $CH_3O(CH_2)_cCH_{2-q}(OCH_3)_{q+1}$ [where *c* is >0 and *q* is 1 or 2], it is the lone ("leftmost") methoxy group that is immobilized rather than one of those in the polymethoxy group at the other extremity of the adsorbed molecule, because this selection affords minimal impedance at the adsorption site and maximal opportunity for dynamic associative interaction with the mobile sorbed-but-not-adsorbed molecules in the gel system.

When dealing with the linear polyethylene oxide ethers having the GMS $H(CH_2)_m(OCH_2CH_2)_eO(CH_2)_nH$ in which *e* is >1, one is also faced with a less obvious option in selectivity, but nevertheless just as pronounced in its effect. Selective adsorption involving an inner oxygen atom will not afford the same adsorbed molecular architecture as that realized when adsorption involves either of the two outer oxygen atoms. Adsorption *via* the latter mode results in an asymmetric orientation with respect to the adsorption site; that is, the $H(CH_2)_mO$ group will lie close to the plane of adsorption, while the remainder $[(CH_2CH_2O)_eO(CH_2)_nH]$ extends away from the anchor site, as shown in Figure a. If this were to be the preferred selectivity when *e* is >1, then the set of $\alpha_{m,e,m}$-values would be markedly dependent upon *m*, as was observed to be the case when $e = 1$ (Figure 2). But if the preferred selectivity involves an inner ether oxygen atom, the adsorbed polyether will assume a more symmetrical molecular orientation, as shown in Figure 4b, because the two segments tethered to the immobilized oxygen atom both contain

one or more ethylene oxide units that serve to extend their respective segments away from the adsorption site, thereby decreasing accordingly the impedance to adsorption of additional ether molecules and presumably also decreasing the sensitivity of $\alpha_{m,e,n}$ on m and n in the respective polymethylene segments that extend from the ethylene oxide segment(s).

It is reasonable to expect, therefore, that the effect on α caused by systematic incrementation of m or n (or both) would be less if the selection leads to a symmetrical molecular architecture in the adsorbed state than if it leads to an asymmetrical architecture. This implies that it should be possible to adjudicate between the alternative adsorption modes by comparing the log α *vs N* linear relationships observed for the set of symmetrical $H(CH_2)_m(OCH_2CH_2)_eO(CH_2)_mH$ ethers for which e is 2 with that observed when e is 1. Our earlier studies involving sorption of polyethers (see Figures 5 & 8 of ref 12 and here in Figures 2 & 3 above) showed that if the molecular architecture adjacent to the oxygen atom at the adsorption site is kept constant in the two series being considered while a second variable, such as m or n, is incremented within its allowable limits, the decrementation constant (D_s) for the respective log α *vs N* linear relationships (eq 1) will be equal; that is, the two linear relationships will be parallel to one another. But if the molecular architecture adjacent to the oxygen atom at the adsorption site is not the same in such comparisons, the two relationships will *not* be parallel. Moreover the slope of the line crossing from one to the other relationship at each value of the second variable (in this case m) will vary linearly with that variable, as shown in Tables 3, 4, and 9−14 in ref 11 and as expressed in eqs 12−22 in that reference. It was shown that $\Delta D_s/\Delta m$ in these D_s *vs m* relationships reflects the change in the molecular architecture adjacent to the adsorption site of the two homologous series being considered as sensitively as the α-values reflect the molecular structure of the adsorbed molecules that comprise these homologous series.[11]

The $\alpha_{m,e,m}$-values deduced for the $H(CH_2)_m(OCH_2CH_2)_eO(CH_2)_mH$ ethers in which e is 1 (srs. no. 3) and e is 2 (srs. no. 6) are recorded in Table 2. The semilog plots of these data *vs* the respective total number ($N = 2m + 3e + 1$; Figure 5) of mass units therein show that the two linear relationships are *not* parallel. The decrementation constant ($D_3 = 0.0909$) at $e = 1$ is almost twice that ($D_6 = 0.0547$) at $e = 2$. Moreover the slopes of the lines (thin straight lines in Figure 5) that cross over from the log α *vs N* linear relationship for srs. no. 3 to that for srs. no. 6 at the same value of m increase with m (from 1 to 8), as expressed by eq 7. The square of the correlation coefficient for the calculated line of best fit to the data points that comprise eq 7 is $r^2 = 0.9988$.

$$\text{slope} = -D_m = -0.0826 + 0.02506m \qquad (7)$$

This means that the magnitude of $\Delta D_m/\Delta m$ caused by a change from $e = 1$ to $e = 2$ (i.e., 3×0.0251) is comparable to those (0.06) observed for the corresponding incremental changes from $q = 2$ down to $q = 0$ in $H(CH_2)_mOCH_{2-q}(CH_3)_q(CH_2)_{m-1}H$ (see Table 15 in ref 11). On the basis of these results it was concluded that in the case of the $H(CH_2)_m(OCH_2CH_2)_eO(CH_2)_nH$ ethers a change in adsorption preference occurs from the asymmetrical mode, characteristic for those series having $e = 0$ or 1 (Figure 4a), to the symmetrical mode (Figure 4b), which is characteristic of those series having $e > 1$.

Although it is of interest to establish whether or not the effect on $\alpha_{m,2,n}$, caused by incrementation of m or n when e is >1, is similar to that noted when e is 0 (Figure 1) and when e is 1 (Figure 2), only one such unsymmetrical ether has been available to us for testing thus far, namely, $CH_3(OCH_2CH_2)_2OC(CH_3)_3$.

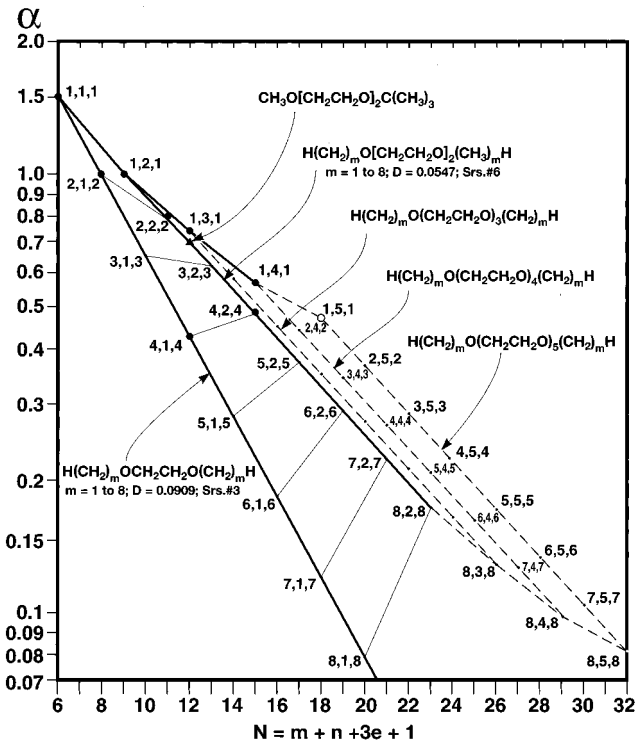

Figure 5. The log α *vs N* relationships for sorption-to-saturation of poly(oxyethylene) ethers $H(CH_2)_mO(CH_2CH_2O)_e(CH_2)_nH$ by poly(Sty-*co*-DVB); correlation of log $\alpha_{m,e,n}$ with N, the sum of methylene (m, $2e$, and n) and oxygen ($e + 1$) mass units in the sorbed ether.

The α-value for this ether (E# 13; Table 1), which is comprised of 12 mass units, is 0.70. It is noteworthy that the data point ($\alpha = 0.70$:$N = 12$; Figure 5) for this ether falls on the line given by the linear log α *vs N* relationship for srs. no. 6, i.e., $H(CH_2)_m(OCH_2CH_2)_2O(CH_2)_mH$. It is inferred from this observation that the decrementation constants for $CH_3(OCH_2CH_2)_2O(CH_2)_nH$, from $n = 1$ to 8, and for $CH_3(OCH_2CH_2)_2OCH_{2-q}(CH_3)_q$, from $q = 1$ to 3, may both be very close to that ($D_6 = 0.0547$) for the symmetrical ethers (srs. no. 6 in Table 2). A trend in this direction was already noted in the comparison of the set of α-values observed for the monoethers R′OR relative to those for the corresponding diethers $R'OCH_2CH_2OR$, as described above. This difference implies that when e becomes greater than 1, the effect on α caused by systematic incrementation of methylene mass units may become independent of the change in molecular architecture caused by the methylene incrementation in the two outer alkyl structures; that is, D_s for such operations may be independent of m, n, or q. If this were indeed true, then it should be possible to deduce the α-values for all the possible permutations of the ethers having GMS $H(CH_2)_{m-1}CH_{2-q'}(CH_3)_{q'}(OCH_2CH_2)_2OCH_{2-q}(CH_3)_q(CH_2)_{n-1}H$, simply by means of eq 1, using $\alpha_{1,2,1} = 1.02$ and $N = 8$ for $CH_3(OCH_2CH_2)_2OCH_3$ (E# 10; Table 1), and $D_6 = 0.0547$ (srs. no. 6; Table 2) for the constants α_i, N_i, and D_s, respectively, because all these α_f-values should fall on the linear log α *vs N* relationship for the triethers having the GMS $H(CH_2)_m(OCH_2CH_2)_2O(CH_2)_mH$ (srs. no. 6; Table 2).

Before one can accept that the above inference is indeed the case for the set of homologous series having $e > 1$, it is necessary to establish at least one more α-value for a member of the series having GMS $CH_3(OCH_2CH_2)_2O(CH_2)_nH$ so that D_s for this homologous series can be established precisely. It is preferable, although not mandatory, that this additional triether be the one having $n = 4$, so that its α-value can be compared directly with that observed for $CH_3(OCH_2CH_2)_2OC(CH_3)_3$ (E#

TABLE 4: The log $\alpha_{1,e,1}$ *vs N* Relationships for the Polyethers Having the GMS $CH_3O[CH_2CH_2O]_eCH_3$ in Which *e* Is Incremented from 1 to 5[a]

m,e,m	$\alpha_{1,e,1}$	*N*	$-D_{e,e+1}$	ΔD_e
1,1,1	**1.50**	6		
1,2,1	**1.02**	9	0.1675	
1,3,1	**0.74**	12	0.1394	0.0281
1,4,1	**0.57**	15	0.1134	0.0260
1,5,1	[0.46]	18	[0.0894]	[0.0240]

[a] Designations 1,1,1; 1,2,1; 1,3,1; and 1,4,1 refer respectively to ethers E#'s 1, 10, 14, and 15; srs. no. 8 in Table 1. $\alpha_{1,e,1}$ is the corresponding adsorption parameter. *N* is the total number of mass units (i.e., $2m + 3e + 1$). $-D_{e,e+1}$ is (log $\alpha_{1,e,1}$ − log $\alpha_{1,e+1,1}$) or 3*D*s = (Δ log α)/ΔN. ΔD_e is the difference [$(-D_e) - (-D_e + 1)$].

13; Table 1). Hopefully one or more of the sought-after polyethers may yet become available to us for swelling studies.

Meanwhile, if one accepts the above inference as a tentative working hypothesis, then one can indicate by analogous reasoning how it is possible to estimate the α-values for all the permutations of the ethers that comprise the corresponding homologous series in which *e* is 3, 4, and 5. To this end, the $\alpha_{1,e,1}$-values for the first four members of the homologous series having the GMS $CH_3(OCH_2CH_2)_eOCH_3$ are recorded in Table 1 (srs. no. 8). These data are correlated in Figure 5 with the corresponding total number ($N = 3e + 3$) of "equivalent" mass units in the polyether, which shows that $\alpha_{1,e,1}$ appears to be decreasing to an asymptotic limit that might be attained before *e* reaches 8. The ratios (log $\alpha_{1,e+1,1}$ − log $\alpha_{1,e,1}$)/($N_{e+1} - N_e$) represent the slopes ($-D_s$, i.e., negative decrementation constants) for the relationships that cross over the log α *vs N* relationships for $H(CH_2)_m(OCH_2CH_2)_eO(CH_2)_mH$ from *e* to *e* + 1 at the same *m* for this set of series in which *m* is incremented from 1 to 8.

The negative slopes of the cross-over relationships ($D_e = 3D_s$) decrease monotonically with *e*, as shown in the second column from the right in Table 4. Moreover the rate of decrease (ΔD_e) is also decreasing monotonically, as shown in the extreme right column, such that it is possible to estimate that the value of $D_{e=5}$ [i.e., (log $\alpha_{1,5,1}$ − log $\alpha_{1,4,1}$) = 0.0894] will be 0.0240 less than $D_{e=4}$ [i.e., (log $\alpha_{1,4,1}$ − log $\alpha_{1,3,1}$) = 0.1134]. The estimated value for $D_{e=5}$ in turn allows one to calculate that the value for $\alpha_{1,5,1}$ will be about 0.46. Each of these three mutually dependent estimated values are bracketed in Table 4 to emphasize that they were obtained by sequential extrapolations as described above.

Although it is possible to extend the extrapolation to the corresponding homologous series of linear poly(oxyethylene) ethers having $e > 5$, in the manner described above, eventually such extrapolations must of necessity become invalid because the ability of the polyether to permeate into cross-linked polystyrene is expected to decrease with increase in chain length simply on the basis of physical size exclusion. This will have a sharp negative effect on $\alpha_{1,e,1}$ at some value of $e > 5$, which will cause marked deviation from the asymptotic trend shown in Figure 5. Moreover, extrapolation beyond $e = 5$ is not necessary for development of the argument that follows in the next two paragraphs.

Despite that the selection of the preferred inner ether oxygen atom in the set of homologous series having GMS $H(CH_2)_m(OCH_2CH_2)_eO(CH_2)_mH$ is expected to change as *e* is incremented from 2 to 5, the molecular architecture adjacent to the oxygen atom immobilized by adsorption will be the same; that is, each segment attached thereto will have one or more ethylene oxide units. Consequently, the log α *vs N* linear relationships having $e = 3$, 4, and 5 will be parallel to that for the series having $e = 2$. These sets of relationships will be displaced from one another, however, by an amount that reflects the monotonic decrease in the respective $\alpha_{1,e,1}$-values, which mark the corresponding data points for the first member in each of these series, as shown in Figure 5. Moreover, the crossover relationships from *e* to $e + 1$ at each value of *m*, from 2 to 8 (not shown in Figure 5 because of space limitations), will be parallel to that noted in Figure 5 for the sequential crossover relationships at $m = 1$; that is, $-D_s = -D_e/3$ at each value of *m* will be equal to (log $\alpha_{1,e,1}$ − log $\alpha_{1,e+1,1}$)/3. Thus, the log $\alpha_{m,e,m}$ *vs N* linear relationships that represent the homologous series in which *e* is 2, 3, 4, and 5 are given by

$$\log \alpha_{m,e,m} = \log \alpha_{1,e,1} - 0.0547(N_m - N_1) \qquad (8)$$

The values for the constants $\alpha_{1,e,1}$ and N_1 at $e = 2$, 3, 4, and 5 are as recorded in Table 4. It is believed tentatively that the $\alpha_{R',e,R}$-values for the polyethers $R'(OCH_2CH_2)_eOR$, in which R′ and R are branched alkyl substituents, can also be calculated using eq 9 and the appropriate values for $\alpha_{1,e,1}$, N_1, and *N* (the total number of equivalent mass units), as discussed previously. Thus, Figure 5 represents a self-consistent multidimensional rigidly interconnected network of log α *vs N* linear relationships (i.e., vectors) for the polyethers that comprise subsets of $R'(OCH_2CH_2)_eOR$. The log α *vs N* linear relationships for the ethers having $e = 1$ are the same as those having the GMS $R'O(CH_2)_cOR$ in which *c* is 2. Consequently the multidimensional system of rigidly interconnected log α *vs N* linear relationships, shown in Figure 5, interfaces with those shown in Figure 3 in the plane designated as plane $\mathbf{A}_2$.

References and Notes

(1) Errede, L. A. Molecular Interpretations of Sorption in Polymers. In *Advances in Polymer Science*; Saegusa, T., Ed.; Springer-Verlag: Berlin−Heidelberg, 1991; Vol. 99.
(2) Errede, L. A. *Macromolecules* **1986**, *19*, 1525.
(3) Errede, L. A. *J. Phys. Chem.* **1989**, *93*, 2668.
(4) Errede, L. A. *J. Phys. Chem.* **1990**, *94*, 466.
(5) Errede, L. A. *J. Phys. Chem.* **1990**, *94*, 3851.
(6) Errede, L. A. *J. Phys. Chem.* **1990**, *94*, 4338.
(7) Errede, L. A. *J. Phys. Chem.* **1991**, *95*, 1836.
(8) Errede, L. A. *J. Phys. Chem.* **1992**, *96*, 3537.
(9) Errede, L. A. *J. Appl. Polym. Sci.* **1994**, *54*, 619.
(10) Errede, L. A. *J. Phys. Chem.* **1994**, *98*, 8580.
(11) Errede, L. A. Polymer Swelling. Part 17: Systematization of steric effects on adsorption parameters as exemplified by swelling to saturation using linear and non-linear acyclic aliphatic ethers. In *Advances in Colloid and Interface Science*; Berg, J., Ed.; Elsevier Science: Amsterdam, 1995; Vol. 61, p 119−198.
(12) Errede, L. A.; Tiers, G. V. D. *J. Phys. Chem.* **1996**, *100*, 9918.
(13) Errede, L. A. *J. Appl. Polym. Sci.* **1992**, *45*, 619.
(14) Tiers, G. V. D. Submitted to *Synthesis*.